Pramana – J. Phys. (2022) 96:110
https://doi.org/10.1007/s12043-022-02358-3
© Indian Academy of Sciences

Influence of pairing symmetry and multiple energy gaps on the behaviour of critical current through the Josephson junction

ORIFJON GANIEV[1,2,3,*], BAKHROM YAVIDOV[4,5] and AZAMAT JALEKESHOV[5]

[1]Institute of Nuclear Physics, Uzbekistan Academy of Sciences, 100214, Tashkent, Uzbekistan
[2]Akfa University, Milliy Bog Street, Tashkent 111221, Uzbekistan
[3]Faculty of Physics, National University of Uzbekistan, 100174, Tashkent, Uzbekistan
[4]Yeoju Technical Institute in Tashkent, 100121, Tashkent, Uzbekistan
[5]Nukus State Pedagogical Institute named after A'jiniyaz, 230105, Nukus, Uzbekistan
*Corresponding author. E-mail: oganiev@yahoo.com

MS received 25 December 2020; revised 27 September 2021; accepted 2 February 2022

Abstract. The extended Ambegaokar–Baratoff model was applied to calculate the critical current (I_c) of a superconductor/insulator/superconductor (S/I/S) Josephson junction with multiple tunnelling channels. We analysed the sensitivity of the critical current, multiplied by normal-state resistance (i.e., I_cR_n product), to the symmetries of the order parameter in the Bardeen–Cooper–Schrieffer (BCS)-type gap formula. In addition, we showed that the temperature dependence of the product $I_cR_n(T)$, which corresponds to multigap symmetry, exhibits a shoulder-like feature and has a pronounced kink at $T \simeq 10$ K for the $SmFeAsO_{0.9}F_{0.1}$ superconductor.

Keywords. Iron-based superconductors; pairing symmetry; critical current; I_cR_n product.

PACS Nos 74.70.Xa; 74.20.Rp; 74.25.Sv; 74.50.+r

1. Introduction

Iron-based superconductors (FeSCs) are a class of high-temperature superconductors synthesised 20 years after the discovery of cuprates, and they are of great interest both from the point of view of fundamental physics and related applications [1–6]. Among the many superconducting properties in these materials, the symmetry of the order parameter plays an important role [7,8]. In this regard, the determination of the gap structure and pairing symmetry is an important step in uncovering the mechanism of iron-based superconductivity and provides a unique chance to understand the high-temperature superconductivity [9,10]. Thus, without a consensus on the pairing symmetry in FeSCs, it is difficult to understand how studying FeSCs can help in understanding the mechanisms of high-temperature superconductivity.

It should be noted that singlet symmetry (i.e., *s*-wave, *d*-wave etc.) on the main members of the FeSC family, including samples of the 1111-, 122-, and 11-type systems was determined by nuclear magnetic resonance (NMR) experiments from Knight shift measurements [11–13]. In addition, multigap symmetry was supported by Josephson tunnelling [14,15], angle-resolved photoemission spectroscopy (ARPES) [15], London penetration [16], impurity doping [17] and scanning tunnelling microscopy (STM) [18] experiments. Among these experiments, the Josephson tunnelling experiment is a powerful method owing to its phase- and amplitude-sensitivity, making it possible to distinguish the multigap from the single gap. In this context, the theoretical study of Josephson tunnelling in recently discovered multigap superconductors, including Fe-pnictides is important to elucidate the type of pairing symmetry.

Theoretical study of multiband superconductors began as a generalisation of the Bardeen–Cooper–Schrieffer (BCS) theory [19] to multigap models, from the works by Suhl *et al* [20], Moskalenko [21] and Kondo [22]. However, the mechanism of superconductivity in the recently discovered FeSCs remain unclear [23–25]. One of the main reason for this is that the pairing symmetry in FeSCs is complex due to the multiband electronic structure. To elucidate the pairing mechanism, it is important to investigate the symmetry of the superconducting phase and then represent the energy and momentum due to the Cooper pairing [24].

Published online: 01 June 2022

In this regard, the work of Nicol and Carbotte [26], using Eliashberg's theory should be noted. In this study, they examined the thermodynamic properties, gap anisotropy and penetration depth for multiband systems, which are possible within the two-band model, as well as identified signatures of their two-band nature have been studied. The authors derived the two-band Eliashberg equations and provided their reduction in the two-square-well approximation, which is needed to identify strong coupling corrections to the renormalised two-band BCS (RBCS). Using microscopic parameters suitable for MgB_2, the authors showed that not only anisotropy, but also strong coupling can have a significant impact, so that the BCS and Eliashberg results can differ significantly in some cases. In addition, it has been reported that anisotropy and strong coupling lead to opposite corrections in most cases. Study of the influence of the interband coupling strength and the rate of interband impurity scattering showed that even a weak interband interaction significantly smears out the transition of the smaller gap band.

In the present work, we study the critical current of a Josephson junction with multiple tunnelling channels due to the multigap structures of superconductors, and analyse the sensitivity of the I_cR_n product curve to the gap symmetry. Based on the experimental data obtained for two-band superconductors, we address the critical current in the superconductor/insulator/superconductor (S/I/S) Josephson junction using the formalism of the Ambegaokar–Baratoff model, within the framework of multiband phenomenology. In particular, to calculate the critical current from the temperature dependence of the self-consistent multiple energy gaps $\Delta_i(T)$ $(i = 1, 2)$, we used the BCS-type model.

2. Theoretical model

When we consider a multiband superconductor, the pair-transfer interactions between different bands (Josephson couplings) are introduced to the Hamiltonian. The multiband BCS model with the attractive interactions is given as

$$H = \sum_{i\sigma} \int \mathrm{d}\mathbf{r}\, \Psi^{\dagger}_{i\sigma}(\mathbf{r}) T_i(\mathbf{r}) \Psi_{i\sigma}(\mathbf{r}) - \sum_{i,j} g_{ij} \int d\mathbf{r}\, \Psi^{\dagger}_{i\uparrow}(\mathbf{r}) \Psi^{\dagger}_{i\downarrow}(\mathbf{r}) \Psi_{j\downarrow}(\mathbf{r}) \Psi_{j\uparrow}(\mathbf{r}), \quad (1)$$

where σ is the spin index $\uparrow$ and $\downarrow$, i and j $(= 1, 2, \ldots)$ are band indices. $T_i(\mathbf{r})$ is the kinetic operator, $\Psi_{j\downarrow}(\mathbf{r})\Psi_{j\uparrow}(\mathbf{r})$ is the band-dependent Cooper-pair amplitude (anomalous average of the field operators with the spin projection up and down for the singlet s-wave pairing). The pairing interaction can be written as

$$\hat{V}_{\mathrm{BCS}} = -\sum_{i,j} g_{ij} \int \mathrm{d}\mathbf{r}\, \Psi^{\dagger}_{i\uparrow}(\mathbf{r}) \Psi^{\dagger}_{i\downarrow}(\mathbf{r}) \Psi_{j\downarrow}(\mathbf{r}) \Psi_{j\uparrow}(\mathbf{r}). \quad (2)$$

It is known that the family of multiband superconducting materials is characterised by the presence of many sheets of the Fermi surface (or bands). In this case, the superconducting properties are controlled by a set of different band condensates [20–22]. Due to the presence of a non-zero interband coupling, such condensates are not independent. As a result, the order parameter of the band, i.e., the measure of condensate in a given band, is not simply proportional to the amplitude of the Cooper pair in this band, but includes the sum over all amplitudes of pairing of bands, each of which is multiplied by a certain coefficient, i.e. coupling constant $g_{ij} = g^*_{ji}$.

Then the total Hamiltonian is transformed to the mean-field form

$$\hat{H}_{\mathrm{MF}} = E_{\mathrm{const}} + \sum_i \int \mathrm{d}\mathbf{r} \Big[\sum_{\sigma} \Psi^{\dagger}_{i\sigma}(\mathbf{r}) T_i(\mathbf{r}) \Psi_{i\sigma}(\mathbf{r}) + \Delta_i(\mathbf{r}) \Psi^{\dagger}_{i\uparrow}(\mathbf{r}) \Psi^{\dagger}_{i\downarrow}(\mathbf{r}) + \Delta^*_i(\mathbf{r}) \Psi_{i\downarrow}(\mathbf{r}) \Psi_{i\uparrow}(\mathbf{r}) \Big]. \quad (3)$$

In the above mean-field Hamiltonian, the gap function in each band is determined by the following expression:

$$\Delta_i(\mathbf{r}) = -\sum_j g_{ij} \langle \Psi_{j\downarrow}(\mathbf{r}) \Psi_{j\uparrow}(\mathbf{r}) \rangle, \quad (4)$$

and its complex conjugate is

$$\Delta^*_i(\mathbf{r}) = -\sum_j g_{ji} \langle \Psi^{\dagger}_{j\uparrow}(\mathbf{r}) \Psi^{\dagger}_{j\uparrow}(\mathbf{r}) \rangle. \quad (5)$$

Next, we derive the corresponding Ginzburg–Landau functional for a two-gap superconductor using eqs (4) and (5). However, it can be assumed that the active band has the strongest pairing interaction $g_{11} = g_1$ in comparison with the interaction in the passive band $g_{22} = g_2$ and with interband scattering of Cooper pairs $g_{12} = g_{21} = g_3$. Then, using eqs (4) and (5), the constant term in Hamiltonian (3) can be expressed in terms of the gap functions as follows [27]:

$$E_{\mathrm{const}} = \frac{1}{G} \int \{ g_2 |\Delta_1|^2 + g_1 |\Delta_2|^2 - g_3 (\Delta^*_1 \Delta_2 + \Delta^*_2 \Delta_1) \}, \quad (6)$$

where G is the matrix of coupling constants equal to $\det\{g_{ij}\} = g_1 g_2 - g_3^2$. When expression (6) has to be modified for $G = 0$, eqs (4) and (5) are linearly dependent. As a result, the ratio of the two gaps

is the same for all temperatures and magnetic fields $\Delta_2(\mathbf{r})/\Delta_1(\mathbf{r}) = g_3/g_1$, while the constant term reduces to $E_{\text{const}} = \int d\mathbf{r}|\Delta_1|^2/g_1$.

In order to define the gap functions, one can apply the standard Gor'kov technique [28] and write the Green's functions as follows:

$$G_{j\sigma\sigma'}(x - x') = -\langle T_\tau \Psi_{j\sigma}(x)\Psi^\dagger_{j\sigma'}(x')\rangle, \tag{7}$$

$$F^+_{j\sigma\sigma'}(x - x') = -\langle T_\tau \Psi^\dagger_{j\sigma}(x)\Psi^\dagger_{j\sigma'}(x')\rangle, \tag{8}$$

where T_τ is the time-ordering operator and $x = (\tau, \mathbf{r})$. In terms of the Green's functions, the gap functions satisfy the system of equations

$$\begin{aligned}\Delta^*_i(\mathbf{r}) &= \sum_j g^*_{ij} F^+_{j\downarrow\uparrow}(\tau' = \tau + 0; \mathbf{r}, \mathbf{r}) \\ &= \sum_j g^*_{ij} \frac{1}{\beta} \sum_n F^+_{j\downarrow\uparrow}(i\omega_n; \mathbf{r}, \mathbf{r}),\end{aligned} \tag{9}$$

where $\beta = k_B T$ and k_B is the Boltzmann constant. The frequencies ω_n are known as the Matsubara frequencies and they depend on temperature. Hence, for fermions (bosons) only odd (even) values of n contribute in the Fourier series, which makes it natural to define

$$\omega_n = \frac{(2n+1)\pi}{\beta}, \quad \text{for fermions,}$$

$$\omega_n = \frac{2n\pi}{\beta}, \quad \text{for bosons.}$$

Thus, the components of the superconducting gap Δ_i are related via the self-consistent equations for a clean superconductor in zero magnetic field and are determined as follows:

$$\Delta_i = \sum_j \lambda_{ij}\Delta_j \int_0^{\hbar\omega_D} \frac{d\varepsilon}{\sqrt{\varepsilon^2 + \Delta_j^2}} \tanh\left(\frac{\sqrt{\varepsilon^2 + \Delta_j^2}}{2k_B T}\right), \tag{10}$$

where $\lambda_{ij} = g_{ij}N_j$ is the dimensionless coupling constant (between i and j components), N_j is the density of states in the j gap and ω_D is the Debye frequency.

The superconducting transition temperature is given by

$$T_c = \frac{2\hbar\omega_D e^{\gamma_E - 1/\lambda}}{k_B \pi}, \tag{11}$$

where γ_E- ($\hbar$-) is the Euler (Plank) constant and λ is the highest eigenvalue of the λ_{ij} matrix:

$$\lambda = \frac{(\lambda_{11} + \lambda_{22})}{2} + \sqrt{\frac{(\lambda_{11} - \lambda_{22})^2}{4} + \lambda_{12}\lambda_{21}}. \tag{12}$$

Here we only consider a two-gap model case, namely, two components, Δ_1 and Δ_2 for the larger and the smaller gap, respectively.

$$\Delta_1 = \sum_{j=1}^{2} \lambda_{1j}\Delta_j \int_0^{\hbar\omega_D} \frac{d\varepsilon}{\sqrt{\varepsilon^2 + \Delta_j^2}} \tanh\left(\frac{\sqrt{\varepsilon^2 + \Delta_j^2}}{2k_B T}\right), \tag{13}$$

$$\Delta_2 = \sum_{j=1}^{2} \lambda_{2j}\Delta_j \int_0^{\hbar\omega_D} \frac{d\varepsilon}{\sqrt{\varepsilon^2 + \Delta_j^2}} \tanh\left(\frac{\sqrt{\varepsilon^2 + \Delta_j^2}}{2k_B T}\right) \tag{14}$$

and $g_{11} = g_1$, $g_{12} = g_{21} = g_3$ and $g_{22} = g_2$, where g_1 and g_2 are the pair interaction constants of the first and second gaps, respectively. g_3 is the interband scattering between Copper pairs of the two gaps. For simplification, we assumed that $\lambda_{12} = \lambda_{21}$.

We then applied the previously calculated superconducting gaps to the Ambegaokar–Baratoff [29] equation for the different tunnelling channels

$$I_c R_n(T) = \sum_i K_i \frac{\pi}{2} \frac{\Delta_i(T)}{e} \tanh\left(\frac{\Delta_i(T)}{2k_B T}\right), \tag{15}$$

where e is the elementary charge, $\Delta_i(T)$ means the i gap of the superconducting order parameters and K_i is the ratio coefficient for the i channel (we note that $\sum_i K_i = 1$). K_1 depends on the curvature near T_c of the critical current curve, which is generally narrow and corresponds to a value smaller than K_2, i.e., the probability of tunnelling though the second channel is much higher than that of the first channel.

3. Numerical results and discussion

Some theoretical models discuss the experimental consequences of an extended s-wave ($s_\pm$-wave) superconductor and the existence of two gaps in iron pnictides for properties related to tunnelling and Josephson junctions. A theoretical model with two gaps and extended s-wave symmetry was discussed by Ota *et al* [30] as a scenario of low critical currents for the intergrain Josephson currents in polycrystalline samples. Incoherent as well as coherent tunnelling processes were taken into account and it was shown that the intergrain Josephson current is significantly reduced by the existence of the interband tunnelling channels, when incoherent tunnelling plays a dominant role. The Ambegaokar–Baratoff relation was extended by Ota *et al* [31] to a hetero (or hybrid) S/I/S Josephson junction with multiple tunnelling channels corresponding to a multigap superconductor coupled to a conventional s-wave superconductor. The differences for s-wave and $s_\pm$-wave symmetry were calculated.

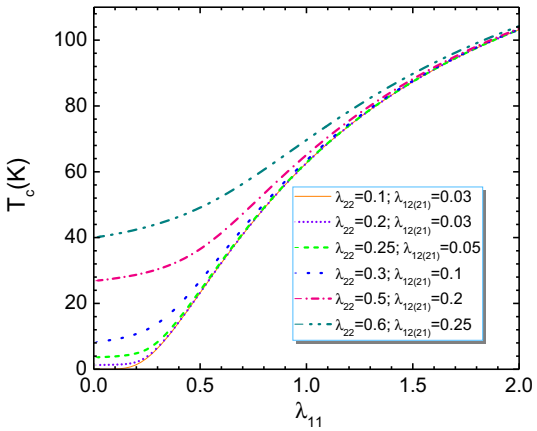

Figure 1. The superconducting transition temperature (T_c) as a function of the intraband coupling λ_{11}.

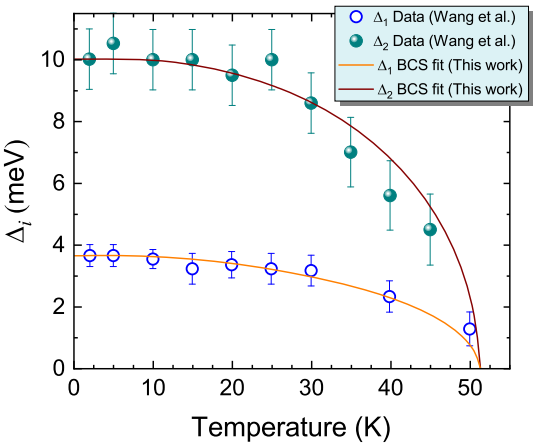

Figure 2. Temperature dependencies of the experimental gap values for $SmFeAsO_{0.9}F_{0.1}$ determined using point-contact spectroscopy data taken from ref. [32] (open and filled circles) and the respective BCS fits (solid lines) within the framework of multiband phenomenology.

Furthermore, it should also be noted that using point contact spectroscopy, the Hai-Hu Wen group reported the observation of two gaps in a polycrystalline sample of $SmFeAsO_{0.9}F_{0.1}$ with the critical temperature for the superconducting transition $T_c = 51.5$ K [32]. They found two order parameters with different energy scales that depend on temperature. Their experimental data were presented as compelling evidence that $SmFeAsO_{0.9}F_{0.1}$ is an unconventional multi-gap superconductor.

The aforementioned experimental and theoretical studies show that to study the influence of the order parameters on the behaviour of the Josephson junction, it is important to know the temperature dependence of the critical current. Therefore, to study the temperature-dependent curves of the critical current, we applied an

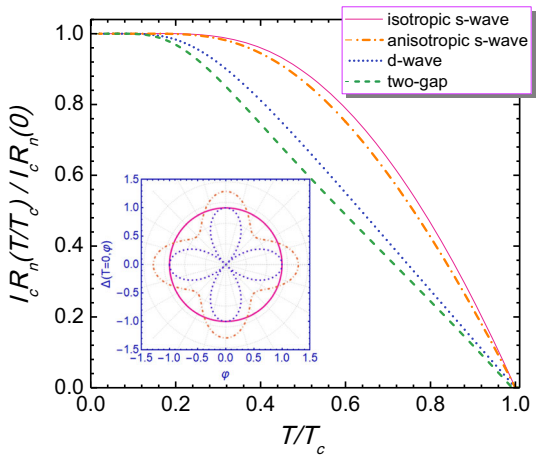

Figure 3. Main panel: I_cR_n product curves, scaled to zero temperature, calculated for various gap symmetries. Inset: Angular part of the superconducting gap on the polar graph for isotropic s-wave symmetry (solid line), anisotropic s-wave symmetry, e.g. $\Delta_s^{An} = 1 + A\cos(4\varphi)$ (dash–dotted line) and d-wave symmetry $\Delta_d = \cos(2\varphi)$ (dotted line), respectively.

effective two-band model to $SmFeAsO_{0.9}F_{0.1}$ superconductor.

First, we examine the superconducting transition temperature T_c as a function of the intraband coupling λ_{11} for the following six cases, when $\omega_D = 150$ meV, namely the combinations: $\lambda_{22} = 0.1$, $\lambda_{12(21)} = 0.03$; $\lambda_{22} = 0.2$, $\lambda_{12(21)} = 0.03$; $\lambda_{22} = 0.25$, $\lambda_{12(21)} = 0.05$; $\lambda_{22} = 0.3$, $\lambda_{12(21)} = 0.1$; $\lambda_{22} = 0.5$, $\lambda_{12(21)} = 0.2$; $\lambda_{22} = 0.6$, $\lambda_{12(21)} = 0.25$. The remarkable and general dependence of T_c on λ_{11} is clearly visible, as T_c remains insignificantly small up to values of $\lambda_{11} = 0.2$ with the exception of the increased interband coupling $\lambda_{12} \gtrsim 0.1$ which also causes small values of λ_{11} to significantly increase in T_c. This theoretical observation demonstrates that the main role in improving T_c belongs to intraband coupling. The increases in T_c can be seen in more detail in figure 1 using the λ_{ij} values.

In figure 2, we show the temperature dependence of both the larger gap and the smaller one described by the prediction of BCS theory. The gap value of $\Delta_0 = 10$ meV leads to $2\Delta_0/k_BT_c = 4.5$, which is a little bit larger than the prediction of weak-coupling d-wave BCS theory. Here, the corresponding parameters for $SmFeAsO_{0.9}F_{0.1}$ superconductor are as follows: $T_c = 51.5$ K; $\lambda_{11} = 1.6521$; $\lambda_{12} = \lambda_{21} = 0.5$; $\lambda_{22} = 0.3033$. Moreover, both gaps are closed around T_c, reflecting the existence of interband coupling in $SmFeAsO_{0.9}F_{0.1}$ superconductor.

Next, based on the numerical data obtained from the self-consistent gap equations, we study the dependence of the product I_cR_n on temperature in the models with different gap symmetries: isotropic s-wave, anisotropic

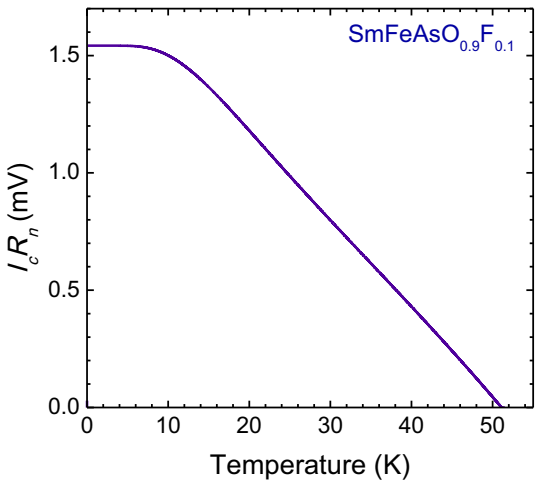

Figure 4. Temperature dependence of the product I_cR_n for $SmFeAsO_{0.9}F_{0.1}$ calculated using the Ambegaokar–Baratoff relation in the framework of the two-gap model.

s-wave, d-wave, as well as for the model with two gaps. The results is presented in the main panel of figure 3 as a dependence of ratio $I_cR_n(T/T_c)/I_cR_n(0)$ on T/T_c (where $I_cR_n(0)$ is the product of I_cR_n at $T = 0$ K). In all the cases of pairing symmetry, the values of the coefficients K_1 and K_2 are equal to 0.2 and 0.8, respectively. As can be seen from the main panel of figure 3, the $I_cR_n(T/T_c)/I_cR_n(0) - T/T_c$ curves for the two-gap model differ from the single gap models in both s-wave and d-wave symmetry due to interband coupling effects. However, the inset in figure 3 shows the angular part of the gap function through isotropic s-wave symmetry, anisotropic s-wave symmetry and d-wave symmetry plotted on the polar graph as a solid line, dash–dotted line and dashed line, respectively. One can notice the appearance of the shoulder-like feature of the curve in the two-gap model. Such a feature is absent in the single-gap models with different wave symmetries.

In figure 4, we present the temperature dependence of the product I_cR_n for $SmFeAsO_{0.9}F_{0.1}$ calculated using the Ambegaokar–Baratoff equation within the framework of the two-gap model for the Josephson tunnelling. In doing this, we use the same values of the coupling constant components λ_{ij}, used for plotting the temperature dependence of the gap function in figure 2. The only thing we assume here is that the probability of tunnelling through the second channel is much higher than that of the first channel, i.e. $K_1 = 0.11$ and $K_2 = 0.89$. This means that the second gap dominates in Josephson tunnelling. It can be seen from figure 4, that the product I_cR_n curve exhibits shoulder-like behaviour in the polycrystalline $SmFeAsO_{0.9}F_{0.1}$ superconductor, and this may be due to the influence of multigap symmetry.

The variation of the temperature-dependent I_cR_n product curves is shown in figure 5 for different values of K_1 and K_2. Indeed, we can conclude on the basis of figure 5, that the critical current at $T_c \simeq 0$ K corresponds to a smaller value when $K_2 > K_1$ (i.e., the probability of tunnelling through the second channel is much higher than that of the first channel) than when $K_1 > K_2$.

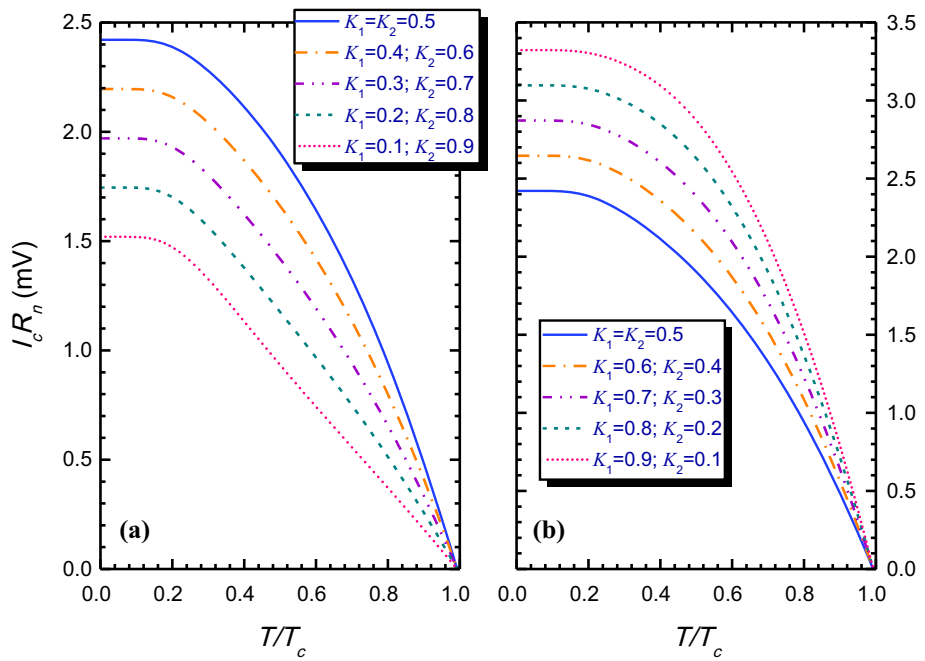

Figure 5. Variation of the temperature-dependent I_cR_n product curves on K_i (where (**a**) $K_1 < K_2$ and (**b**) $K_1 > K_2$) calculated using the Ambegaokar–Baratoff relation in the framework of the two-gap model.

4. Conclusion

In summary, a two-band model is presented to describe the critical current behaviour of a S/I/S Josephson junction with multiple tunnelling channels. Within the framework of this model, two energy gaps with different energy scales were used to analyse the experimental data of Wang *et al* [32] obtained using point contact spectroscopy. It is shown that the temperature dependence of the product $I_c R_n$ exhibits shoulder-like behaviour and has a pronounced kink at $T \simeq 10$ K. This behaviour is the specific feature of the presented model, in particular, the model with two effective energy gaps with different magnitudes. Our theoretical study performed within the framework of multi-band phenomenology provides a strong evidence that $SmFeAsO_{0.9}F_{0.1}$ is an unconventional superconductor with multiple energy gaps.

Acknowledgements

The authors are grateful to the Ministry of Innovative Development of Uzbekistan (M.I.D.U.), for financial support in the implementation of this research work.

References

[1] H Hosono, K Tanabe, E Takayama-Muromachi, H Kageyama, S Yamanaka, H Kumakura, M Nohara, H Hiramatsu and S Fujitsu, *Sci. Technol. Adv. Mater.* **16**, 033503 (2015)
[2] H Hosono and K Kuroki, *Physica C* **514**, 399 (2015)
[3] Q Si, R Yu and E Abrahams, *Nat. Rev. Mater.* **1**, 16017 (2016)
[4] H Hosono, A Yamamoto, H Hiramatsu and Y Ma, *Mater. Today* **21**, 278 (2018)
[5] C Yao and Y Ma, *Supercond. Sci. Technol.* **32**, 023002 (2019)
[6] S J Singh and P Mele, *Future potential of new high T_c iron-based superconductors* (Springer, Cham, 2020)
[7] P J Hirschfeld, M M Korshunov and I I Mazin, *Rep. Prog. Phys.* **74**, 124508 (2011)
[8] H-H Wen and S Li, *Annu. Rev. Condens. Matter Phys.* **2**, 121 (2011)
[9] A Chubukov, *Annu. Rev. Condens. Matter Phys.* **3**, 57 (2012)
[10] P J Hirschfeld, *Compt. Rend. Phys.* **17**, 197 (2016)
[11] H-J Grafe *et al*, *Phys. Rev. Lett.* **101**, 047003 (2008)
[12] S Onari, H Kontani and Y Tanaka, *J. Phys. Soc. Jpn.* **77**, 023703 (2008)
[13] Y Shimizu, T Yamada, T Takami, S Niitaka, H Takagi and M Itoh, *J. Phys. Soc. Jpn.* **78**, 123709 (2009)
[14] C T Chen, C C Tsuei, M B Ketchen, Z A Ren and Z X Zhao, *Nat. Phys.* **6**, 260 (2010)
[15] P Richard, T Sato, K Nakayama, T Takahashi and H Ding, *Rep. Prog. Phys.* **74**, 124512 (2011)
[16] R T Gordon *et al*, *Phys. Rev. Lett.* **102**, 127004 (2009)
[17] J Li *et al*, *Phys. Rev. B* **85**, 214509 (2012)
[18] H Yang, Z Wang, D Fang, Q Deng, Q H Wang, Y Y Xiang, Y Yang and H-H Wen, *Nat. Commun.* **4**, 2749 (2013)
[19] J Bardeen, L Cooper and R Schrieffer, *Phys. Rev.* **106**, 162 (1957)
[20] H Suhl, B T Matthias and L R Walker, *Phys. Rev. Lett.* **3**, 552 (1959)
[21] V A Moskalenko, *Phys. Met. Metallogr.* **8**, 25 (1959)
[22] J Kondo, *Prog. Theor. Phys.* **29**, 1 (1963)
[23] Y Kamihara, H Hiramatsu, M Hirano, R Kawamura, H Yanagi, T Kamiya and H Hosono, *J. Am. Chem. Soc.* **128**, 10012 (2006)
[24] Y Kamihara, T Watanabe, M Hirano and H Hosono, *J. Am. Chem. Soc.* **130**, 3296 (2008)
[25] J Paglione and R L Greene, *Nat. Phys.* **6**, 645 (2010)
[26] E J Nicol and J P Carbotte, *Phys. Rev. B* **71**, 054501 (2005)
[27] M E Zhitomirsky and V H Dao, *Phys. Rev. B* **69**, 054508 (2004)
[28] L P Gor'kov, *J. Exp. Theor. Phys.* **36**, 1918 (1959); translated in *Sov. Phys. JETP* **9**, 1364 (1959)
[29] V Ambegaokar and A Baratoff, *Phys. Rev. Lett.* **10**, 486 (1963)
[30] Y Ota, M Machida, T Koyama and H Matsumoto, *Phys. Rev. Lett.* **102**, 237003 (2009)
[31] Y Ota, N Nakai, H Nakamura, M Machida, D Inotani, Y Ohashi, T Koyama and H Matsumoto, *Phys. Rev. B* **81**, 214511 (2010)
[32] Y -L Wang, L Shan, L Fang, P Cheng, C Ren and H-H Wen, *Supercond. Sci. Technol.* **22**, 015018 (2009)